IEEE Access
Multidisciplinary Rapid Review Open Access Journal

Received April 10, 2017, accepted May 22, 2017, date of publication June 1, 2017, date of current version June 28, 2017.

Digital Object Identifier 10.1109/ACCESS.2017.2710212

Sparse Extension Array Geometry for DOA Estimation With Nested MIMO Radar

WANG ZHENG[1], XIAOFEI ZHANG[1,2], AND JUNPENG SHI[1,3]

[1]College of Electronic Information Engineering, Nanjing University of Aeronautics and Astronautics, Nanjing 210000, China
[2]State Key Laboratory of Millimeter Waves, Southeast University, Nanjing 210096, China
[3]Air and Missile Defense College, Air Force Engineering University, Xi'an 710051, China

Corresponding author: Xiaofei Zhang (fei_zxf@163.com)

This work was supported in part by the China NSF under Grant 61371169, Grant 61601167, and Grant 61601504, in part by the Open Research Fund of National Mobile Communications Research Laboratory, Southeast University, under Grant 2015D030, in part by the Jiangsu NSF under Grant BK20161489, in part by the Open Research Fund of State Key Laboratory of Millimeter Waves, Southeast University, under Grant K201826, and in part by the Fundamental Research Funds for the Central Universities under Grant NE2017103.

ABSTRACT The two-level nested array geometry, which systematically nests two uniform linear subarrays, is proved to offer $O(N^2)$ degrees of freedom (DOFs) with only N sensors. In this paper, a novel sparse extension array geometry for nested multiple-input multiple-output radar is proposed to provide $O(N^4)$ DOFs with N sensors. In the proposed geometry, both the transmitter and receiver are equipped with the two-level nested arrays, where we particularly extend the inter-element spacing of the transmitter with a sparse extension factor, leading to a great increase of DOF. Furthermore, we derive the closed-form expressions for the sensor locations and the available DOFs. Spatial smoothing-based MUSIC algorithm is employed to validate the effectiveness and superiority of the proposed sparse extension array for direction of arrival estimation.

INDEX TERMS Sparse extension, nested array, monostatic multiple-input multiple-output (MIMO) radar, degree of freedom (DOF).

I. INTRODUCTION

As multiple-input multiple-output (MIMO) radars employ multiple physical sensors to simultaneously transmit independent waveforms and exploit multiple physical sensors to receive the reflected signals [1], [2], they possess plenty of advantages over traditional phased-array radars [3], e.g., parameter identifiability improvement [4], higher degrees of freedom (DOFs) [5] and better estimation accuracy [6]. As a typical issue for MIMO radar systems, direction of arrival (DOA) estimation has been extensively studied in the past decades. In [7], estimation of signal parameters via rotational invariance technique (ESPRIT) algorithm was applied to MIMO radar systems by utilizing the rotational invariance property between the transmitter and receiver for DOA estimation. An ESPRIT- based algorithm for MIMO radar [8] was proposed to alleviate the complexity but with negligible performance degeneration. A novel method, called conjugate ESPRIT [9], was proposed to detect more signals than the methods in [7] and [8] by using the reduced-dimension transformation and property of noncircular signals. However, all the aforementioned MIMO radar configurations are equipped with the uniform linear arrays (ULAs) in the transmitter and receiver, where the inter-element spacing is limited to half-wavelength to avoid phase ambiguity problem [10].

In general, the maximum number of targets that can be detected exploiting an N sensors ULA with popular subspace algorithms, e.g., multiple signal classification (MUSIC) and ESPRIT [11], [12], is $N-1$. Nowadays, several sparse arrays have been proposed to increase the DOFs and resolve more sources than the number of sensors, e.g., the minimum redundancy arrays (MRAs) [13], coprime arrays [14] and nested arrays [15]. The minimum redundancy (MR) was extended to monostatic MIMO radar for an increasing DOF [16], whereas an exhaustive search is involved to solve the optimization problem of the designing for MR MIMO radar. Unlike the monostatic MIMO radar in [16] with the transmitter and receiver separated in parallel, a different type of monostatic MIMO radar [17] was employed to increase the DOFs and decrease the computational search. A nested MIMO system was exploited [18] to estimate the DOAs of uncorrelated and coherent targets. Nevertheless, the aforementioned geometries simply place the sparse arrays in both the transmitter and receiver, where the resultant co-arrays can generally provide $O(N^2)$ DOFs [16], [18] or $O(N^3)$ DOFs [17] with N sensors.

In this paper, by utilizing the generalized nested array, a sparse extension array geometry with nested MIMO radar is proposed to enhance the DOFs. Essentially, in the proposed geometry, both the transmitter and receiver are equipped with the two-level nested arrays, and the inter-element spacing of the transmitter is extended with a sparse extension factor. Based on the difference and sum co-arrays, it is proved that the proposed geometry can achieve $O(N^4)$ DOFs with N sensors. Moreover, we provide the closed-form expressions for the sensor locations and the achievable DOFs. And spatial smoothing MUSIC (SS-MUSIC) algorithm [15] is employed to validate the effectiveness and superiority of the proposed sparse extension array.

To be more specific, the main contributions of this paper can be summarized as: 1) We construct a sparse extension array geometry with nested MIMO radar using the generalized nested array and specifically the total number of DOFs can reach $O(N^4)$ with N sensors, while the existing geometries in [16]–[18] can only provide $O(N^2)$ or $O(N^3)$ DOFs; 2). We derive the closed-form expressions for the maximum number of DOFs and the sensor locations of the transmitter and receiver while the MR MIMO radar [16] involves an exhaustive search for optimal geometries.

The rest of this paper is organized as follows. The data model of the nested MIMO radar is presented in Section II. In Section III, we present the proposed sparse extension array. Section IV provides the numerical simulations and Section V concludes the paper.

Notation: We use lower-case (upper-case) bold characters to denote vectors (matrix). $(\cdot)^T$, $(\cdot)^*$, $(\cdot)^H$ respectively denote the transpose, the conjugate, the conjugate transpose of a vector or matrix. $\otimes$ represents the Kronecker product and $\circ$ is the Khatri-Rao product. $vec(\cdot)$ stands for the vectorization process that stacks the columns of a matrix. $diag\{\cdot\}$ represents the diagonal operation.

II. DATA MODEL

Consider a nested MIMO radar consisting of a receiver with M sensors and a transmitter with N sensors, where the receiver and transmitter are closely located so that the far-field targets impinge on the two arrays with the same angles. Assume that there are K far-field uncorrelated narrowband targets from the directions $\{\theta_k, k = 1, 2, \cdots, K\}$, where the positions of receiver are $\Phi_R = \{d_{rm}|m = 1, 2, \cdots, M\}$ and positions of transmitter are $\Phi_T = \{d_{tn}|n = 1, 2, \cdots, N\}$. Note that in this paper, we suppose that K is already known. An example of the nested MIMO radar [18] is shown in Fig. 1, where $M = 2$ and $N = 3$.

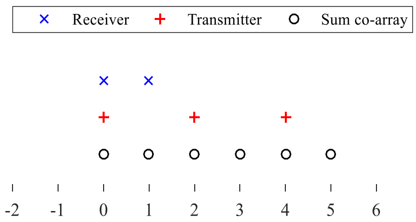

FIGURE 1. The example of nested MIMO and its sum co-array.

The output of the matched filters for the received signal can be represented as [5]

$$\begin{aligned}\mathbf{x}(t) &= [\mathbf{a}_t(\theta_1) \otimes \mathbf{a}_r(\theta_1), \cdots, \mathbf{a}_t(\theta_K) \otimes \mathbf{a}_r(\theta_K)]\, \mathbf{s}(t) + \mathbf{n}(t) \\ &= \mathbf{A}\mathbf{s}(t) + \mathbf{n}(t), \end{aligned} \tag{1}$$

where $\mathbf{s}(t) = [s_1(t), s_2(t), \cdots, s_K(t)]^T \in \mathbb{C}^{K\times 1}$, $\mathbf{n}(t) \in \mathbb{C}^{NM\times 1}$ is the white Gaussian noise vector with zero mean and variance σ_n^2 and $\mathbf{A} = [\mathbf{a}_t(\theta_1) \otimes \mathbf{a}_r(\theta_1), \cdots, \mathbf{a}_t(\theta_K) \otimes \mathbf{a}_r(\theta_K)]$ · $\mathbf{a}_t(\theta_k)$ and $\mathbf{a}_r(\theta_k)$ are the steering vectors of the transmitter and receiver for the k-th target, which can be expressed as

$$\mathbf{a}_t(\theta_k) = \left[e^{j2\pi d_{t1}\sin\theta_k/\lambda}, \cdots, e^{j2\pi d_{tN}\sin\theta_k/\lambda}\right]^T, \tag{2}$$

$$\mathbf{a}_r(\theta_k) = \left[e^{j2\pi d_{r1}\sin\theta_k/\lambda}, \cdots, e^{j2\pi d_{rM}\sin\theta_k/\lambda}\right]^T, \tag{3}$$

where λ stands for the wavelength, $d_{tn} \in \Phi_T$ is the sensor location in the transmitter and $d_{rm} \in \Phi_R$ is the sensor position in the receiver. And the covariance matrix can be obtained by

$$\mathbf{R}_x = E[\mathbf{x}\mathbf{x}^H] = \mathbf{A}\mathbf{R}_s\mathbf{A}^H + \sigma_n^2\mathbf{I}, \tag{4}$$

where $\mathbf{R}_s = diag\{\sigma_1^2, \sigma_2^2, \cdots, \sigma_K^2\}$ and σ_k^2 is the power of the k-th target. In practice, the covariance matrix is obtained with finite number of snapshots, $\hat{\mathbf{R}}_x = (1/L)\sum_{t=1}^{L} \mathbf{x}(t)\mathbf{x}(t)^H$, where L is the total number of snapshots.

We vectorize the covariance matrix in (4) and the observing vector can be represented by [15]

$$\begin{aligned}\mathbf{z} &= vec(\mathbf{R}_x) = (\mathbf{A}^* \circ \mathbf{A})\mathbf{p} + \sigma_n^2\mathbf{e} \\ &= \mathbf{B}\mathbf{p} + \sigma_n^2\mathbf{e}, \end{aligned} \tag{5}$$

where $\mathbf{e} = [\mathbf{e}_1^T, \mathbf{e}_2^T, \cdots, \mathbf{e}_{NM}^T]^T$, $\mathbf{e}_i \in \mathbb{R}^{NM\times 1}$ is a vector consisting of zeros except a number 1 at the i-th position ($i = 1, 2, \cdots, NM$), $\mathbf{p} = [\sigma_1^2, \sigma_2^2, \cdots, \sigma_K^2]^T$ and $\mathbf{B} = (\mathbf{A}^* \circ \mathbf{A}) = [\mathbf{b}(\theta_1), \mathbf{b}(\theta_2), \cdots, \mathbf{b}(\theta_K)]$.

$$\mathbf{b}(\theta_k) = [\mathbf{a}_t(\theta_k) \otimes \mathbf{a}_r(\theta_k)]^* \otimes [\mathbf{a}_t(\theta_k) \otimes \mathbf{a}_r(\theta_k)], \tag{6}$$

where $k = 1, 2, \cdots, K$.

III. SPARSE EXTENSION ARRAY GEOMETRY

In this section, we first make a brief review of difference co-array and sum co-array. Then the proposed sparse extension array is presented and the closed-form expression for available DOFs is derived.

A. REVIEW

Definition 1 (Difference Co-Array): The difference co-array of a linear array has the positions represented by the unique elements of the set S_{dc}, which can be defined as follow [15]:

$$S_{dc} = \{u - u', u, u' \in S_u\}. \tag{7}$$

where S_u denotes the set of physical sensor locations.

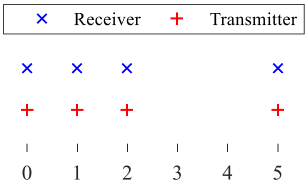

FIGURE 2. An example of NA-TR for nested MIMO radar.

Definition 2 (Sum Co-Array): The sum co-array of a pair of linear arrays has the positions given by the unique elements of the set S_{sc}, which can be obtained by [18]

$$S_{sc} = \{u_1 + u_2, u_1 \in S_1; u_2 \in S_2\}, \tag{8}$$

where S_1 and S_2 are the physical sensor positions of the two linear arrays.

B. SPARSE EXTENSION ARRAY GEOMETRY

According to (6), the resulting co-array of the nested MIMO radar has the positions given by the unique elements of the set

$$\begin{aligned} S_{nested} &= \left\{-d_t' - d_r' + d_t'' + d_r'' | d_t', d_t'' \in \Phi_T; d_r', d_r'' \in \Phi_R\right\} \\ &= \left\{(d_t'' - d_t') + (d_r'' - d_r') | d_t', d_t'' \in \Phi_T; d_r', d_r'' \in \Phi_R\right\} \\ &= \{\mu_t + \mu_r | \mu_t \in \Psi_T; \mu_r \in \Psi_R\}, \end{aligned} \tag{9}$$

where Ψ_T is the difference co-array set of the transmitter and Ψ_R is the difference co-array set of the receiver. Specifically, the resulting co-array of the nested MIMO radar can be regarded as the sum co-array of two difference co-arrays.

As the algorithms devised for traditional monostatic MIMO radar with ULAs for both the transmitter and receiver have been widely investigated and, in particular, the difference co-array of the two-level nested array is a filled ULA [15], a reasonable trivial MIMO geometry for nested MIMO radar consists of typical two-level nested arrays for both the transmitter and receiver (NA-TR), then the existing algorithms can be employed. And the array sensors in the transmitter and receiver are located at

$$\begin{aligned} \Omega_T &= \{n_1 d_{t1} | n_1 = 0, 1, \cdots, N_1 - 1\} \\ &\quad \cup \{N_1 \lambda/2 + n_2 d_{t2} | n_2 = 0, 1, \cdots, N_2 - 1\}, \end{aligned} \tag{10}$$

$$\begin{aligned} \Omega_R &= \{m_1 d_{r1} | m_1 = 0, 1, \cdots, M_1 - 1\} \\ &\quad \cup \{M_1 \lambda/2 + m_2 d_{r2} | m_2 = 0, 1, \cdots, M_2 - 1\}, \end{aligned} \tag{11}$$

where $d_{t1} = d_{r1} = \lambda/2$, $d_{t2} = (N_1 + 1)d_{t1}$ and $d_{r2} = (M_1 + 1)d_{r1}$, $M = M_1 + M_2$, $N = N_1 + N_2$. According to [15], the difference co-arrays of the transmitter and the receiver are both ULAs with $2N_2(N_1+1)-1$ and $2M_2(M_1+1)-1$ sensors respectively and the positions are given by

$$L_{T\_dc} = \{p\lambda/2 | p = -P, \cdots, P, P = N_2(N_1 + 1) - 1\}, \tag{12}$$

$$L_{R\_dc} = \{q\lambda/2 | q = -Q, \cdots, Q, Q = M_2(M_1+1) - 1\}, \tag{13}$$

where L_{T_dc} is the difference co-array set of the transmitter and L_{R_dc} is the difference co-array set of the receiver. An example of NA-TR geometry for nested MIMO radar is shown in Fig. 2, where $N_1 = N_2 = 2$, $M_1 = M_2 = 2$.

However, this scheme for nested MIMO radar can generally provide $O(N_1N_2+M_1M_2)$ DOFs with $(N_1+N_2+M_1+M_2)$ sensors. In the following part, based on the trivial scheme above, we present the sparse extension array geometry with a sparse extension factor, which leads to an impressive increase of DOF and $O(N_1N_2M_1M_2)$ DOFs can be achieved with the $(N_1 + N_2 + M_1 + M_2)$ sensors.

Consider that the transmitter and receiver of nested MIMO radar consist of two-level nested arrays, where the transmitter has $N = N_1 + N_2$ sensors and the receiver has $M = M_1 + M_2$ sensors. Different from the trivial NA-TR geometry with typical two-level nested arrays, we specifically enlarge the inter-element spacing of the transmitter with a sparse extension factor α and the sensor positions are provided by

$$\begin{aligned} \Omega_T^\alpha &= \alpha \Omega_T \\ &= \{n_1 \alpha d_{t1} | n_1 = 0, 1, \cdots, N_1 - 1\} \\ &\quad \cup \{N_1 \alpha \lambda/2 + n_2 \alpha d_{t2} | n_2 = 0, 1, \cdots, N_2 - 1\}, \end{aligned} \tag{14}$$

where α is a positive integer within the set $[1, 2, \cdots, 2M_2(M_1+1)-1]$. It can be observed that the difference co-array of the transmitter is still a filled ULA, whereas the inter-element spacing of the ULA is also enlarged by α and the positions are given by the following set

$$\begin{aligned} L_{T\_dc}^\alpha &= \alpha L_{T\_dc} \\ &= \{p\alpha\lambda/2 | p = -P, \cdots, P, P = N_2(N_1+1) - 1\}. \end{aligned} \tag{15}$$

Proposition: For the proposed sparse extension array geometry, (i). The maximum number of the filled co-array is $2\alpha[N_2(N_1 + 1) - 1] + 2M_2(M_1 + 1) - 1$.

(ii). The positions of the filled co-array are given by

$$\begin{aligned} \{v\lambda/2 | v = -V, \cdots, V, V \\ = \alpha[N_2(N_1 + 1) - 1] + M_2(M_1 + 1) - 1\}. \end{aligned}$$

Proof: When the sparse extension factor takes the integer within the set $[1, 2, \cdots, 2M_2(M_1 + 1) - 1]$, similar to [15] and [18], a consecutive ULA can be obtained without holes. As a result, combining (13) and (15), the boundaries of the resulting co-array can be attained.

For the left boundary,

$$\begin{aligned} &-[M_2(M_1 + 1) - 1] + [-\alpha N_2(N_1 + 1) + \alpha] \\ &\quad = -\alpha[N_2(N_1 + 1) - 1] - M_2(M_1 + 1) + 1 = -V. \end{aligned} \tag{16}$$

For the right boundary,

$$\begin{aligned} &[M_2(M_1 + 1) - 1] + [\alpha N_2(N_1 + 1) - \alpha] \\ &\quad = \alpha[N_2(N_1 + 1) - 1] + M_2(M_1 + 1) - 1 = V. \end{aligned} \tag{17}$$

And the maximum number of the consecutive co-array is $2\alpha[N_2(N_1 + 1) - 1] + 2M_2(M_1 + 1) - 1$.

Remark: According to (12)-(13), the difference co-arrays of the transmitter and receiver are both ULAs. On the basis of the nested MIMO system in [18], for the difference co-array of the transmitter, the spacing can be $[2M_2(M_1 + 1) - 1]\lambda/2$, where $2M_2(M_1+1)-1$ is the sensor number of the difference co-array of the receiver. Also the sparse extension factor can

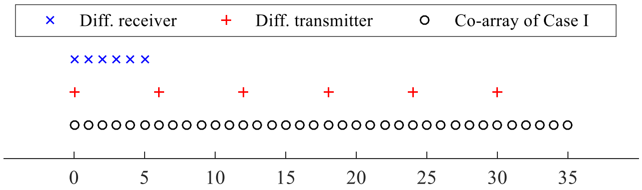

FIGURE 3. An example of Case I.

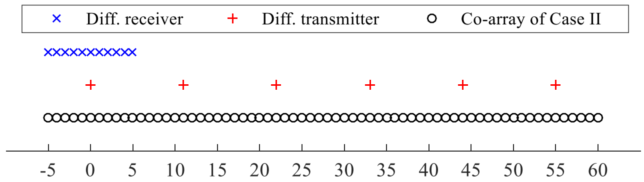

FIGURE 4. An example of Case II.

take the values smaller than $2M_2(M_1+1)-1$. However, as the redundancies increase, the total number of DOFs decreases. Specifically, Case II can be regarded as the generalization of the uniform MIMO radar [16], which will be derived in the next part.

To better illustrate the proposed sparse extension array, we will provide two special cases as examples below.

1) Case I ($\alpha = M_2(M_1+1)$)

Comparing (13) and (15), as the two difference co-arrays of the transmitter and receiver in the proposed geometry are both symmetric about the *zero*-th position, we only take the positive parts into consideration for simplicity. In Case I, we enlarge the inter-element spacing of the transmitter with a sparse extension factor $\alpha = M_2(M_1+1)$, which consequently enlarge the inter- element spacing of the difference co-array of the transmitter. And specifically, α is equal to the number of the positive difference co-array of the receiver (including the sensor at the *zero*-th position). Fig. 3 captures the two difference co-arrays of Case I, where we set $N_1 = N_2 = 2$ and $M_1 = M_2 = 2$.

The resultant positive sum co-array of Case I contains a filled ULA with $N_2M_2(N_1+1)(M_1+1)$ sensors, where the positions are $L_I^+ = \{r\lambda/2 | r = 0, 1, \cdots, R_1, R_1 = N_2M_2(N_1+1)(M_1+1)-1\}$ and the sensor positions of the corresponding negative sum co-array are given by $L_I^- = -L_I^+$. In summary, the resultant co-array of Case I consists of a filled ULA with $2N_2M_2(N_1+1)(M_1+1)-1$ sensors, which means that Case I can provide $2N_2M_2(N_1+1)(M_1+1)-1$ DOFs.

2) Case II ($\alpha = 2M_2(M_1+1)-1$)

In the case $\alpha > M_2(M_1+1)$, holes [19] will arise if we only take the positive part of the difference co-arrays. As an enhancement of Case I, we consider the positive difference co-array of the transmitter and the whole difference co-array of the receiver, where the holes can be filled and a ULA can be obtained. In Case II, the inter-element spacing of the transmitter is enlarged with sparse extension factor $\alpha = 2M_2(M_1+1)-1$ which is equal to the sensor number in the whole difference co-array of the receiver. Fig. 4 depicts an example of Case II, where $N_1 = N_2 = 2$ and $M_1 = M_2 = 2$.

In summary, the resulting co-array of Case II is a filled ULA with $2N_2M_2(N_1+1)(M_1+1) - N_2(N_1+1)$ sensors and the sensor position set is represented as $L_{II}^+ = \{s\lambda/2 | s = -R_3, \cdots, R_2\}$, where $R_2 = [N_2(N_1+1)-1][2M_2(M_1+1)-1] + M_2(M_1+1)-1$, $R_3 = M_2(M_1+1)-1$, and the mirrored position set is given by $L_{II}^- = -L_{II}^+$. The total achievable DOF of Case II is $[2N_2(N_1+1)-1][2M_2(M_1+1)-1]$. Fig. 5 illustrates the sparse extension array geometry, the difference co-arrays of the transmitter and receiver and the resulting co-array of Case II, which shows clearly that the resulting co-array is a much longer filled ULA, where $N_1 = N_2 = 2$ and $M_1 = M_2 = 2$.

According to *Proposition* (*i*), Case II is capable of attaining the maximum number of DOF, where $\alpha = 2M_2(M_1+1)-1$, as the maximum number of DOF is linear versus sparse extension factor α. When given the total number of sensors T, to achieve the maximum number of DOF, we can construct the following optimization problem

$$\begin{aligned} &\max \;\; [2N_2(N_1+1)-1][2M_2(M_1+1)-1] \\ &s.t.\; T = N_1+N_2+M_1+M_2. \end{aligned} \tag{18}$$

The Lagrange function of (18) can be represented as

$$\begin{aligned} f = {} & [2N_2(N_1+1)-1][2M_2(M_1+1)-1] \\ & + \beta(N_1+N_2+M_1+M_2-T), \end{aligned} \tag{19}$$

where β denotes the Lagrange multiplier. By performing differential calculation on (19), we can obtain

$$N_1+N_2+M_1+M_2-T = 0, \tag{20.a}$$
$$2N_2[2M_2(M_1+1)-1]+\beta = 0, \tag{20.b}$$
$$2(N_1+1)[2M_2(M_1+1)-1]+\beta = 0, \tag{20.c}$$
$$2M_2[2N_2(N_1+1)-1]+\beta = 0, \tag{20.d}$$
$$2(M_1+1)[2N_2(N_1+1)-1]+\beta = 0. \tag{20.e}$$

By solving (20), we can get $N_2 = N_1+1 = (T+2)/4$, $M_2 = M_1+1$ and $N_2 = M_2$, the maximum DOF is

$$\mathrm{DOF}_{\max} = \left[\frac{(T+2)^2}{8} - 1\right]^2, \tag{21}$$

where $T = 4k+2$, $k \in \mathbb{Z}^+$. Since T is an arbitrary integer, the other cases are given by the following corollary.

Corollary: Assuming the total number of sensors is T,

(*i*) if $T = 4k$, $k \in \mathbb{Z}^+$, $N_1 = N_2 = M_1 = M_2 = T/4$;

(*ii*) if $T = 4k+1$, $k \in \mathbb{Z}^+$, $N_1 = N_2 = M_1 = M_2 - 1 = (T-1)/4$ or $N_1 = N_2 - 1 = M_1 = M_2 = (T-1)/4$;

(*iii*) if $T = 4k+3$, $k \in \mathbb{Z}^+$, $N_1 + 1 = N_2 = M_1 = M_2 = (T+1)/4$ or $N_1 = N_2 = M_1 + 1 = M_2 = (T+1)/4$.

In Table I, the DOFs of the nested MIMO system [18], NA-TR, Case I and Case II are listed with a given number

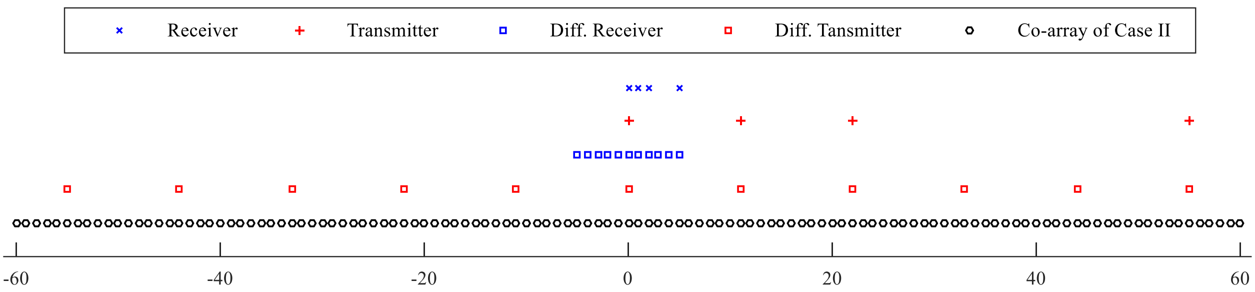

FIGURE 5. An example of the sparse extension array geometry (Case II).

TABLE 1. The DOFs of different geometries.

Sensor number	NA-TR	Nested MIMO	Case I	Case II
10	33	25	161	289
14	61	49	511	961
18	97	81	1249	2401

of sensors, where NA-TR and the nested MIMO in [18] both select the case of the maximum number for DOF. It shows clearly that the proposed two cases can achieve a significant increase of DOF.

Note that the final resultant co-arrays of the two cases are both filled ULAs whose spacing is half-wavelength, which means no ambiguity problem presents and the subspace-based algorithms [15] or sparse representation method [20] can be utilized for DOA estimation directly.

IV. SIMULATION RESULTS

In this section, numerical simulations are provided to validate the effectiveness and superiority of the proposed sparse extension array geometry. We consider that the receiver consists of a typical two-level nested array with $M = 4$ sensors ($M_1 = M_2 = 2$). For Case I, the transmitter is composed of a two-level nested array exploiting sparse extension with $N = 4$ sensors ($N_1 = N_2 = 2$), where $d'_{t1} = 6\lambda/2$, $d'_{t2} = 18\lambda/2$. And for Case II, the transmitter is made up of $N = 4$ sensors ($N_1 = N_2 = 2$), where $d''_{t1} = 11\lambda/2$ and $d''_{t2} = 33\lambda/2$. The total number of sensors is 8. As the performance metric, root mean square error (RMSE) is employed, i.e.,

$$RMSE = \sqrt{\frac{1}{K\Gamma}\left(\sum_{\tau=1}^{\Gamma}\sum_{k=1}^{K}(\theta_k - \hat{\theta}_{k,\tau})^2\right)}, \quad (22)$$

where Γ is the number of Monte-Carlo simulations and $\hat{\theta}_{k,\tau}$ stands for the τ-th trial of the k-th angle θ_k. Specifically, we set $\Gamma = 500$.

A. MUSIC SPECTRUM

In Fig. 6, the numerical examples are presented to verify the number of available DOFs based on SS technique [15]. As the nested MIMO system [18] can attain at most 16 DOFs with 4 sensors ULA for both the transmitter and receiver, the two cases of the proposed sparse extension array can respectively obtain 71 DOFs for Case I and 121 DOFs for Case II. For better illustration, we assume there are $K = 25$ far-filed uncorrelated narrowband targets uniformly distributed within $[-60°, 60°]$ impinging on the antennas, where $L = 1000$ and SNR = 5dB. It is shown clearly in Figs. 6 that by exploiting SS-MUSIC, the proposed two sparse extension arrays can detect all the targets, whereas the nested MIMO system can resolve no more than 15 targets. It depicts clearly in Fig.6 that the spectrum peaks of Case II are sharper than those of Case I as Case II can provide more DOFs and simultaneously the array aperture of Case II is extended more than Case I.

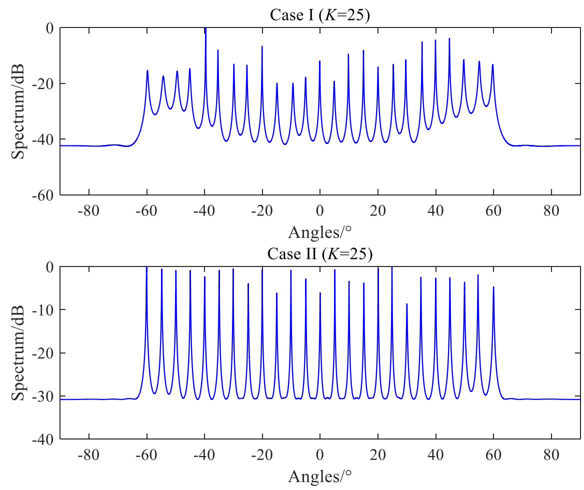

FIGURE 6. Spatial spectrum with SS-MUSIC.

B. RMSE PERFORMANCE VERSUS SNR AND SNAPSHOTS

We employ SS-MUSIC to study the RMSE performance of DOA estimation with the proposed two array geometries versus SNR and snapshots. In addition, the NA-TR, the nested MIMO system [18], and a traditional monostatic MIMO radar with ULAs on both the transmitter and receiver [8] are provided for comparison. All the geometries in this simulation are made up of 8 sensors for fair comparison. We assume there are $K = 3$ targets impinging on the antennas from the elevation angles $[10°, 30°, 50°]$. Fig. 7 captures the RMSE

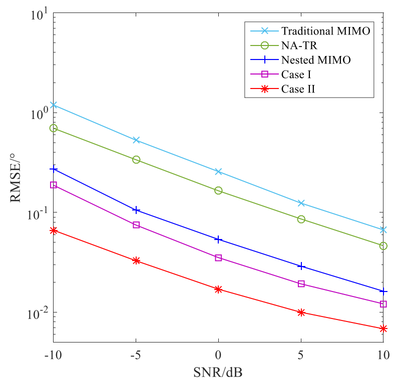

FIGURE 7. RMSE of different geometries versus SNR.

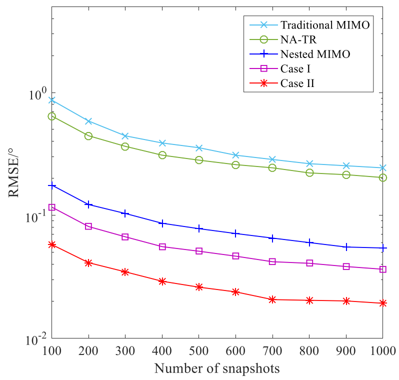

FIGURE 8. RMSE of different geometries versus snapshots.

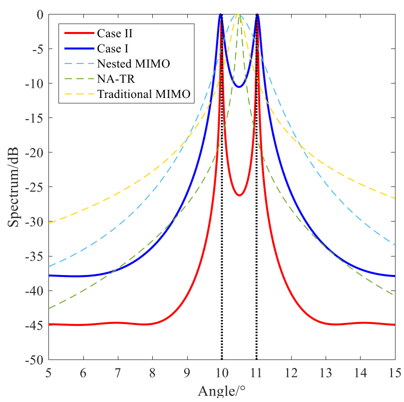

FIGURE 9. SS-MUSIC spectrum with two closely located targets.

performance of SS- MUSIC with different geometries versus SNR, where $L = 1000$, while Fig. 8 illustrates the DOA estimation performance of SS- MUSIC with different geometries by varying the number of snapshots and SNR = 0dB. From these two figures, it is shown that the performance of all the examples improves with SNR or the number of snapshots increasing. Specifically, the two cases of the proposed sparse extension array outperform the others due to a larger array aperture.

C. RESOLUTION PERFORMANCE

In this simulation, suppose that there are two targets impinging on the antennas from θ_1 and θ_2, where the estimates of the

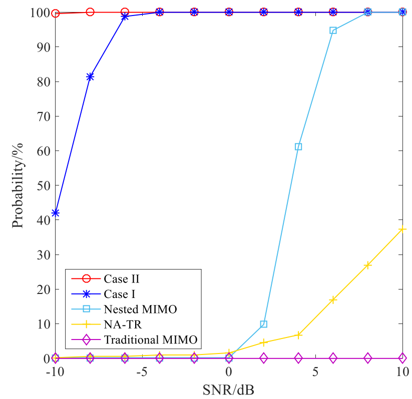

FIGURE 10. Estimation probability versus SNR with $L = 200$.

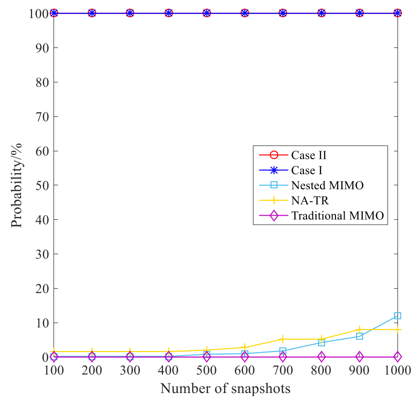

FIGURE 11. Estimation probability versus snapshots with SNR = 0dB.

two angles are denoted by $\hat{\theta}_1$ and $\hat{\theta}_2$. The two targets can be resolved if $|\theta_1 - \hat{\theta}_1| < |\theta_1 - \theta_2|/2$ and $|\theta_2 - \hat{\theta}_2| < |\theta_1 - \theta_2|/2$. Fig. 9 depicts the SS-MUSIC spectrum of the 5 geometries, where the number of sensors is the same as Fig.7, $\theta_1 = 10°$, $\theta_2 = 11°$ and $L = 1000$, SNR = 10dB. It shows clearly that SS-MUSIC algorithm only with the proposed sparse extension array can distinguish the two targets. To study the estimation probability of the 5 geometries with SS-MUSIC, we select another group of targets with $\theta_1 = 10°$ and $\theta_3 = 12°$. Fig. 10 and Fig. 11 show the estimation probability of the 5 geometries versus SNR and snapshots respectively. In conclusion, as the array aperture has been extended greatly, the proposed sparse extension array has better performance than the other three geometries.

V. CONCLUSION

In this paper, a sparse extension array geometry with nested MIMO radar by using the generalized nested array structure is proposed, which exploits N sensors to provide $O(N^4)$ DOFs. In the proposed geometry, both the transmitter and receiver consist of the two-level nested arrays. And the inter-element spacing of the transmitter is extended with a sparse extension factor, leading to an impressive increase of DOFs. Furthermore, we derive the closed-form expressions for the sensor locations and the achievable DOFs. The effectiveness and superiority of the proposed sparse extension array are validated with SS- MUSIC.

REFERENCES

[1] E. Fishler, A. Haimovich, R. Blum, D. Chizhik, L. Cimini, and R. Valenzuela, "MIMO radar: An idea whose time has come," in *Proc. IEEE Radar Conf.*, Philadelphia, PA, USA, Apr. 2004, pp. 71–78.

[2] J. Li and P. Stoica, "MIMO radar—Diversity means superiority," in *Proc. 14th Adapt. Sensor Array Process Workshop (ASAPW)*, Dec. 2006, pp. 1–6.

[3] E. Brookner, "Phased-array radars," *Sci. Amer.*, vol. 252, no. 2, pp. 94–102, 1988.

[4] J. Li, P. Stoica, L. Xu, and W. Roberts, "On parameter identifiability of MIMO radar," *IEEE Signal Process. Lett.*, vol. 14, no. 12, pp. 968–971, Dec. 2007.

[5] I. Bekkerman and J. Tabrikian, "Target detection and localization using MIMO radars and sonars," *IEEE Trans. Signal Process.*, vol. 54, no. 10, pp. 3873–3883, Oct. 2006.

[6] E. Fishler, A. Haimovich, R. S. Blum, L. J. Cimini, D. Chizhik, and R. A. Valenzuela, "Spatial diversity in radars-models and detection performance," *IEEE Trans. Signal Process.*, vol. 54, no. 3, pp. 823–838, Mar. 2006.

[7] C. Duofang, C. Baixiao, and Q. Guodong, "Angle estimation using ESPRIT in MIMO radar," *Electron. Lett.*, vol. 44, no. 12, pp. 770–771, Jun. 2008.

[8] X. Zhang and D. Xu, "Low-complexity ESPRIT-based DOA estimation for colocated MIMO radar using reduced-dimension transformation," *Electron. Lett.*, vol. 47, no. 4, pp. 283–284, 2011.

[9] W. Wang, X. Wang, H. Song, and Y. Ma, "Conjugate ESPRIT for DOA estimation in monostatic MIMO radar," *Signal Process.*, vol. 93, no. 7, pp. 2070–2075, 2013.

[10] C. Zhou, Z. Shi, Y. Gu, and X. Shen, "DECOM: DOA estimation with combined MUSIC for coprime array," in *Proc. IEEE Int. Conf. Wireless Commun. Signal Process.*, Oct. 2013, pp. 1–5.

[11] R. O. Schmidt, "Multiple emitter location and signal parameter estimation," *IEEE Trans. Antennas Propag.*, vol. 34, no. 3, pp. 276–280, Mar. 1986.

[12] R. Roy and T. Kailath, "ESPRIT-estimation of signal parameters via rotational invariance techniques," *IEEE Trans. Acoust., Speech, Signal Process.*, vol. 37, no. 7, pp. 984–995, Jul. 1989.

[13] A. Moffet, "Minimum-redundancy linear arrays," *IEEE Trans. Antennas Propag.*, vol. 16, no. 2, pp. 172–175, Mar. 1968.

[14] P. P. Vaidyanathan and P. Pal, "Sparse sensing with co-prime samplers and arrays," *IEEE Trans. Signal Process.*, vol. 59, no. 2, pp. 573–586, Feb. 2011.

[15] P. Pal and P. P. Vaidyanathan, "Nested arrays: A novel approach to array processing with enhanced degrees of freedom," *IEEE Trans. Signal Process.*, vol. 58, no. 8, pp. 4167–4181, Aug. 2010.

[16] C.-Y. Chen and P. P. Vaidyanathan, "Minimum redundancy MIMO radars," in *Proc. IEEE Int. Symp. Circuits Syst. (ISCAS)*, May 2008, pp. 45–48.

[17] Y. Huang, G. Liao, J. Li, J. Li, and H. Wang, "Sum and difference coarray based MIMO radar array optimization with its application for DOA estimation," *Multidimensional Syst. Signal Process.*, pp. 1–20, Feb. 2016.

[18] S. Qin, Y. D. Zhang, and M. G. Amin, "DOA estimation of mixed coherent and uncorrelated signals exploiting a nested MIMO system," in *Proc. IEEE Benjamin Franklin Symp. Microw. Antenna Sub-Syst.*, Philadelphia, PA, USA, Sep. 2014, pp. 1–3.

[19] S. Qin, Y. D. Zhang, and M. G. Amin, "Generalized coprime array configurations for direction-of-arrival estimation," *IEEE Trans. Signal Process.*, vol. 63, no. 6, pp. 1377–1390, Mar. 2015.

[20] N. Hu, Z. Ye, X. Xu, and M. Bao, "DOA estimation for sparse array via sparse signal reconstruction," *IEEE Trans. Aerosp. Electron. Syst.*, vol. 49, no. 2, pp. 760–773, Apr. 2013.

WANG ZHENG, photograph and biography not available at the time of publication.

XIAOFEI ZHANG, photograph and biography not available at the time of publication.

JUNPENG SHI, photograph and biography not available at the time of publication.